Research Article
Neck Moment Response Characterization of Restrained Child Occupant at Standard Test Impact Speed 24.4 km/h

[1,2]S. Shasthri, [3]V. Kausalyah, [1]Q.H. Shah, [1]K.A. Abdullah, [1]M. M. Idres and [4]S.V. Wong
[1]Faculty of Engineering, International Islamic University Malaysia, 50728 Kuala Lumpur, Malaysia
[2]Faculty of Engineering, Universiti Selangor, 40000 Shah Alam, Selangor, Malaysia
[3]Faculty of Mechanical Engineering, Universiti Teknologi MARA, 40000, Selangor, Malaysia
[4]Malaysian Institute of Road Safety Research (MIROS), Kajang 43000, Selangor, Malaysia

Abstract: The effects of bullet vehicle crash impact angle, child restraint system design and restraint harness slack at standard test side impact speed of 24.4 km/h (15 mph) on moments sustained at the neck by a three year old child is investigated. A statistical methodology employing the Design of Experiments is adopted in this study whereby a Latin Hypercube Sampling is chosen as the experiment design. Mathematical models are built using the Response Surface Method based on simulation results whereby, good fitness is achieved. The singular and cross interactive effect of each predictor on the neck moment is analyzed. The number of significant parameters affecting the Neck Moment is shown to be largest for wide impact angles ($\phi \geq 60°$). The vehicle impact angle parameter is revealed to be the largely the most sensitive parameter and on which all the other remaining parameters are highly dependent on. An ideal safe range for low neck moments has been established to be within ϕ angles 42° and 60°. The vehicle impact angle parameter is shown to be proportional to neck moments for wide impact angles, while it behaves inversely proportional to neck moments for narrow impact angles. The other parameters are generally found to be moderately significant only for wide impact angles. The harness friction coefficient is shown to hold relatively very little influence on neck moments.

Keywords: Child neck moment, child restraint system, lateral impact, principle degree of force, response surface method, vehicle crash

INTRODUCTION

It has been shown, over the last two decades, that vehicle crashes has become the leading cause of death for children in developed countries (NHTSA, 2005; Statistics Canada, 2003). The side impact crash mode especially is shown to be a particularly harmful mode (Starnes and Eigen, 2002; Decina and Knoebel, 1996). Many factors contribute to this scenario, one of which is the presence of shoulder harness slack (Decina and Knoebel, 1996). Another is due to the kinematics of side impact crash which depends upon both the magnitude of the impulse from the bullet vehicle, as well as its Principle Direction of Force (PDOF) impacting angle (Anderson et al., 2011). In addition, it has been shown that that head contact with intruding door due to the bullet vehicle, plays a pivotal role as well and has to be considered in addressing any mitigation efforts (Howard et al., 2004; Arbogast et al., 2005).

Although head injuries is largely reported to be prime cause of fatalities in Child Restraint System (CRS) restrained toddlers involved in side impact crash (Arbogast et al., 2004; Arbogast et al., 2005), However there is sufficient cause for concern where the fatality may also be related to high neck loading (Weber, 2000). Investigation of Neck Moments pertaining to CRS design, misuse and crash parameters is yet unexplored due to insufficient accident data and costly full vehicle analysis simulations. Thus, the effects and relationships between the singular and cross interactive parameters, especially for oblique side impact involving intrusion are not studied (Arbogast et al., 2005). Insights obtained from such a work would serve to promote better understanding of the side impact crash event in order to achieve greater injury mitigation.

In this study, a study is undertaken to characterize the Neck Moment (NM) of a CRS restrained 3 year old child occupant involved in lateral and oblique side impact, with respect to identified relevant crash parameters. A Prescribed Structural Motion (PSM) simulation is carried out where a pre-validated Hybrid model consisting of both Finite Elements (FE) and Multi-bodies (Mb) is subjected to a pulse, which represents the bullet vehicle kinematic impact load. The

Corresponding Author: S. Shasthri, Department of Mechanical Engineering, Faculty of Engineering, International Islamic Universiti Malaysia, 50728 Kuala Lumpur, Malaysia

methodology allows for significant savings in computational cost while preserving the required accuracy. MADYMO 7.4.1 by TASS is used for the simulation due to its capability to handle both FE and MB. A Design of Experiments (DoE) using the Latin Hypercube Sampling (LHS) is employed to build mathematical models using the Response Surface Method (RSM). Statistical methods are used to map the parameter sensitivity upon the NM both individually as well as cross interactively. Statistical modeling and analysis is conducted using MATLAB 2013a. The present work reports data corresponding to a bullet vehicle at standard testing impact speed of 24.4 km/h (15 mph).

METHODOLOGY

Numerical modelling: An R44-standard compliant CRS is modelled using shell elements with a specified thickness of 4 mm. The material property is defined as polypropylene. The density (ρ), Young's modulus (E) and Poisson's ratio (μ) are specified respectively as 800 kg/m^3, 0.842 GPa and 0.3 whereas the yield and the ultimate tensile strengths are set as 8.76 and 18.76 MPa respectively (NHTSA, 2007; Kapoor *et al*., 2008; Wang *et al*., 2007). A foam insert comprising of solid elements is also modelled as shown in Fig. 1. This is placed at the side wings of the CRS to absorb head impact. A highly compressible low-density foam material model (ρ = 50.2 kg/m^3, E = 5.463 MPa) is used (Kapoor *et al*., 2008; Wang *et al*., 2007). The CRS is constrained at base anchorage points on a ECE R.44 test bench using fixed cross bars.

The five-point harness system of the CRS is modelled predominantly using 1 mm thick membrane elements (ρ = 890.6 kg/m^3, E = 2.068 GPa, μ = 0.3). However, to reduce computation time, the FE belts are connected at both ends to the anchor point using rigid bodies. Loading and unloading data with hysteresis is provided for both belt types (Kapoor *et al*., 2008; Wang *et al*., 2007; TNO, 2013). No slack is allowed for the belt fitting (NHTSA, 2007).

An intrusion of 280 mm is considered (Heiko *et al*., 2007; ECE R95-Reg 95, Year) and this is achieved by means of introducing rigid static planar-surfaces as shown in Fig. 1. The secondary intrusion plane (130 mm intrusion) has contact defined against the CRS as well as the child dummy where else for the primary intrusion plane, only the head is allowed contact with it. This arrangement is assumed to cater for the worst case scenario of the intrusion whereby the head is free to strike the hardest part of the intruding door, at the earliest moment of time.

A commercially available ellipsoid Hybrid III 3YO child dummy model is used in this study (TNO, 2013). Both dummy and CRS are subjected to gravitational loading as well as acceleration pulse to simulate lateral side-impact. The standard acceleration pulse TRC 327 is used as the prescribed motion condition to simulate a lateral side impact of 24.4 km/h (15 mph) impact speed
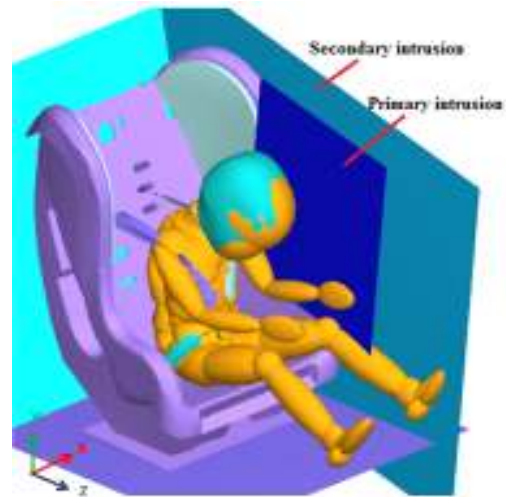

Fig. 1: Oblique side impact PSM simulation

Table 1: DOE grouping and parameter bounds

Attributes	Group	
	PDOF A	PDOF B
X_1 (90°-ϕ) (degrees)	0°≤X_1≤30°	30°≤X_1≤60°
X_2 (degrees)	8°≤X_1≤24°	
X_3 (mm)	3.5≤X_1≤5.5	
X_4 (value)	0.25≤X_1≤0.35	
X_5 (cm)	0≤X_1≤5	
X_6 (cm)	0≤X_1≤5	
Pulse	32.2 km/h (TRC595)	

(NHTSA, 2007). Dynamic simulation time is set to terminate after 125 msec. Convergence study is carried out during the trial runs and a good trade-off between model cost and accuracy is achieved with an element count of 24,320. The entire model assembly has been previously validated and it has been shown to be both accurate as well as computationally economical with each run typically taking only 20 min (Shasthri *et al*., 2013).

Statistical modelling: Figure 2 illustrates the parameters selected for the sensitivity study and Table 1 shows organization of the DoE as well as the upper and lower bounds considered for each parameter adopted from standards (FMVSS, 2013; NHTSA, 2002). To further increase the sensitivity of the study, the PDOF impact angle (ϕ) is divided into two groups, namely PDOF A (60°≤ϕ≤90°) and PDOF B (30°≤ϕ≤60°). The first caters for a wide PDOF angle (ϕ≥60°) impact approach while the later represents a narrow impact approach (ϕ≤60°). The ensuing NM response plots generated by MADYMO are recorded. Multinomial Regression is used as a method to determine parameter sensitivity and hence a quadratic Response Surface Method (RSM) is used to model the problem. The response data is converted to logarithmic values of base 10 and submitted for Regression Analysis.

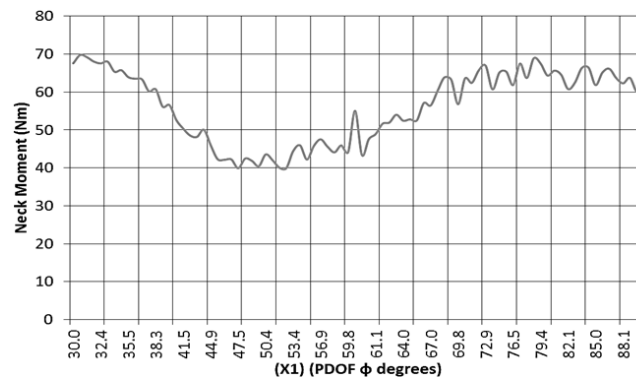Fig. 2: CRS parameters considered for oblique side impact model

Fig. 3: Effect of impact angle parameter X1 on neck moment

Table 2: Model fitness diagnostic statistics

| | Model fitness statistics | | | | |
| | Fisher test | | | | |
RSM models	F statistic[1]	p-value	R^2	R^2 Adj.	RMSE
PDOF A	73.545	4.787E-11	0.9930	0.9795	0.004
PDOF B	29.263	2.5109E-8	0.9826	0.9490	0.025

[1]: F statistic >1.92 to satisfy null hypothesis requirement

RESULTS AND DISCUSSION

From the DoE tabulations, the full range of X_1 values encompassing both PDOF A and B groups against the NM response is plotted as shown in Fig. 3. The values seem to peak at 30° with approximately 70 Nm. A favorable low Neck Moment of 50 Nm and below seems to be indicated between PDOF φ angles 42° and 60°. The NM severity range (approximately above 60 Nm) is indicated for PDOF impact angles less than 39° and greater than 68°. Table 2 shows the statistical diagnostics obtained for all four models. From the regression coefficients, a good fitness is indicated for all the models where the model errors are shown to be low as given by the small RMSE values. The R^2 and R^2 adjusted (R^2 Adj.) values substantiate this conclusion as well as providing a good indication of the model fitness with all values approaching unity. Additionally, results from the Fisher (F) test reconfirm that the RSM models are statistically acceptable and this is supported by the low associated p values.

Student's t-test is used to identify the major contributing single parameters and cross interaction parameters, as well as to assess their respective
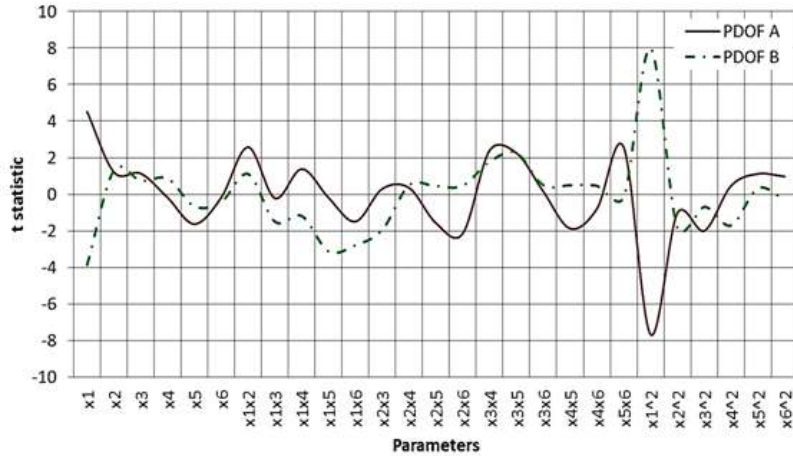
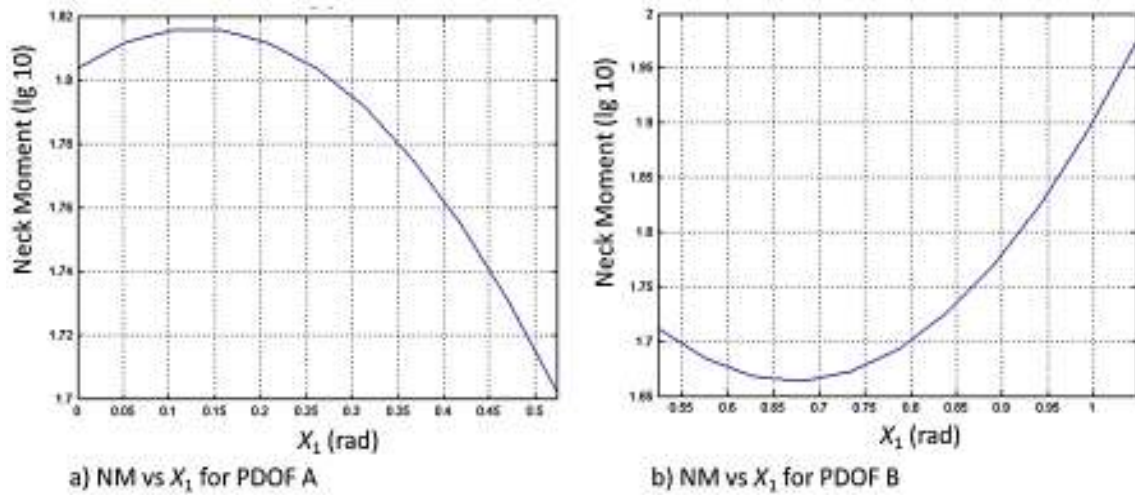Fig. 4: Qualitative analysis of neck moment response for RS models

a) NM vs X_1 for PDOF A

b) NM vs X_1 for PDOF B

Fig. 5: NM significant singular X_1 parameter response line plots

Table 3: t-test and significance p of parameters for neck moment response

Significant parameters*	15 PDOF A		15 PDOF B	
	t	p	t	p
X_1	4.5150	0.0005	-3.8615	0.0017
X_1X_2	2.5775	0.0219		
X_1X_5			-3.1269	0.0074
X_1X_6			-2.7876	0.0145
X_2X_6	-2.1478	0.0497		
X_3X_4	2.3885	0.0316		
X_3X_5	2.2547	0.0407		
X_5X_6	2.5656	0.0224		
X_1^2			7.9792	1.41E-6

*: Only parameters having p value of less than 0.05 are included in the table

parametric significance. Figure 4 depicts the full data distribution and pattern of the t statistic values for each model in graphical form while Table 3 shows the t statistics for only the significant parameters identified.

A quick glance reveals that the PDOF A groups obviously register more number of significant parameters than the PDOF B groups. This shows that

the NM of the restrained 3 year old child during side impact is very much affected by the designated parameters both individually and cross interactively for wide PDOF impact angles of $\phi \geq 60°$. A scrutiny of Table 3 and Fig. 4 reveal the PDOF impact angle ϕ (X_1) to be the most sensitive parameter for all cases, both singularly and cross interactively. Singularly, the significance is found to be especially pronounced for wide PDOF impact angles ($\phi \geq 60°$). It is interesting to note that contrary to PDOF A, values for PDOF B ($\phi \leq 60°$) are negative indicating that increase in X_1 serves only to reduce NM. The Response Surface line plots for X_1 with respect to NM for both impact angle groups are shown in Fig. 5.

Cross interactively, the parameters X_1X_5 and X_1X_6 registers moderate significance for PDOF B although this observation is not seen to hold for wider impact angles (PDOF A). The latter is seen to have a single cross interaction with X_2. No interaction with parameter X_4 is seen for any of the models. The Response Surface
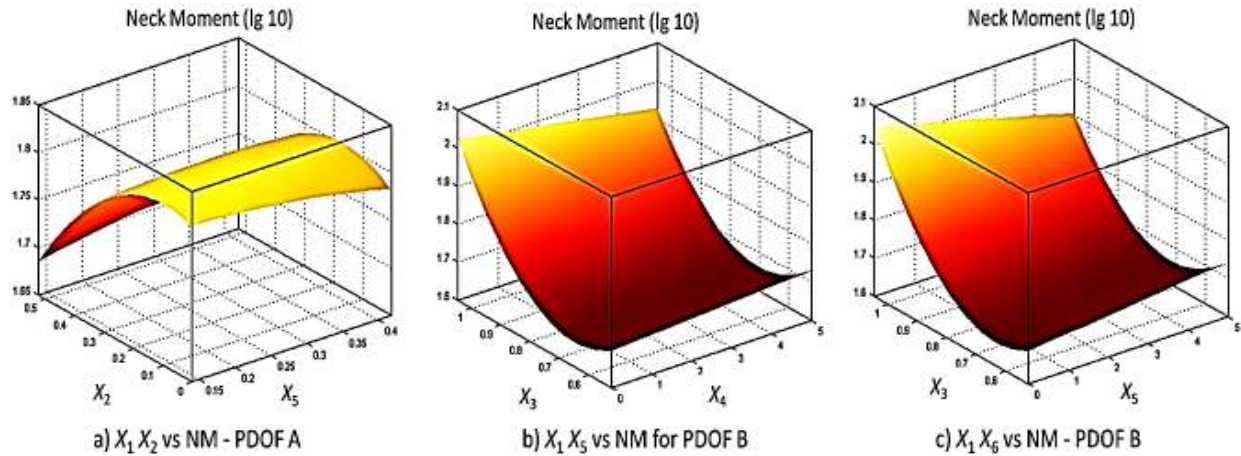
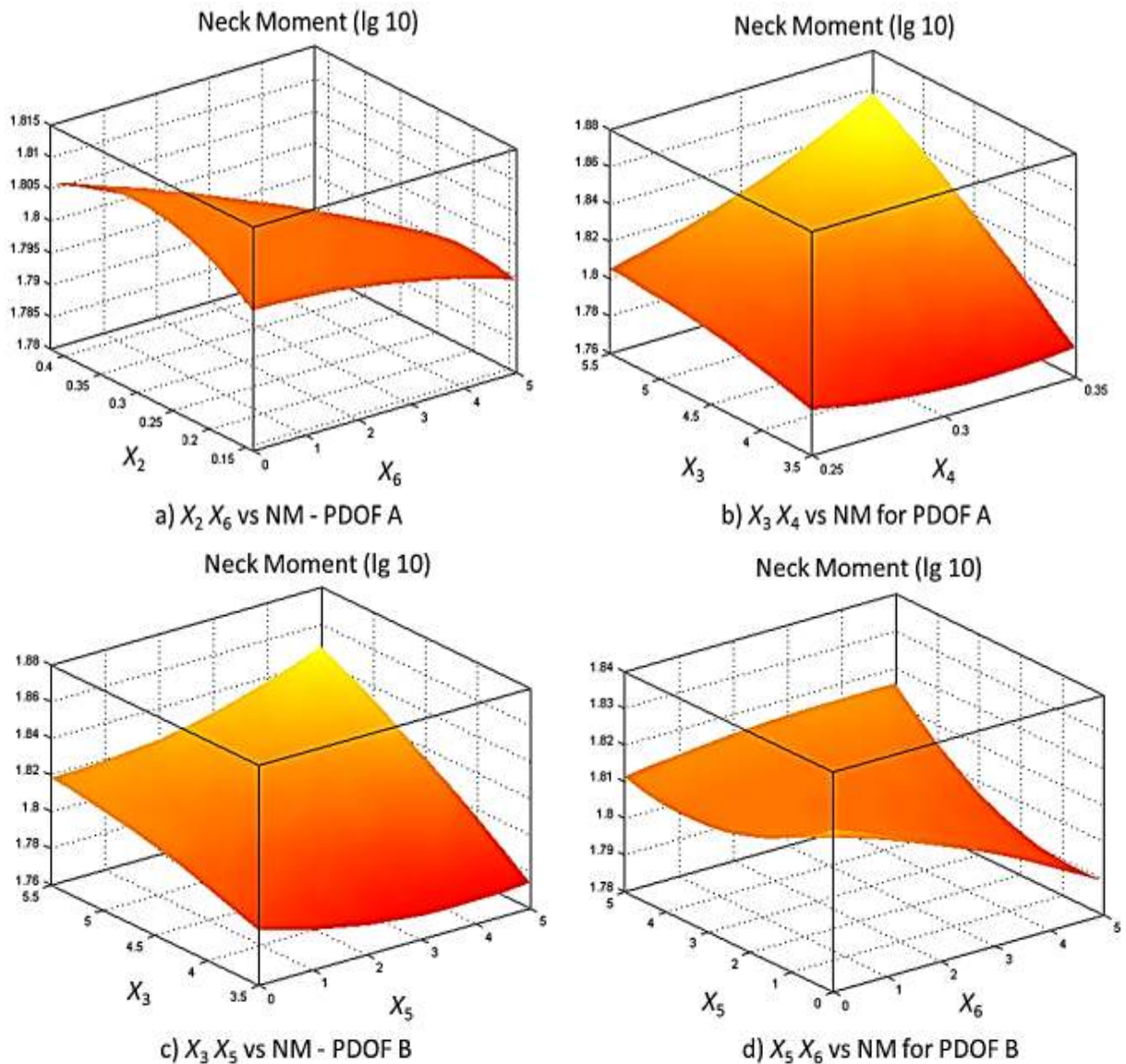Fig. 6: NM significant X_1 cross interactive parameter response surface plots

Fig. 7: NM other significant cross interactive parameter response surface plots

plots for these significant interactions with X_1 are depicted in Fig. 6. The remaining other six parameter significant cross interaction Response Surface plots are given in Fig. 7. The CRS pitch angle parameter (X_2) is found to be sensitive only for wide PDOF impact angles (ϕ≥60°). Singularly, there is no significance, while cross interactively, observations are seen with X_1 (Fig. 6a) and with X_6 (Fig. 7a). Interestingly, for wide PDOF impact angles, the interaction between the CRS pitch angle and the far side harness slack parameter is shown to be of import in reducing NM. The CRS shell thickness parameter X_3 is also similarly shown to have no singular significance but cross interactively noteworthy with X_3X_4 (Fig. 7b) and X_3X_5 (Fig. 7c) for wide PDOF impact Angles (PDOF A) alone.

The harness coefficient of friction parameter X_4 indicates the least sensitivity in this study with only a single positive cross interaction with X_3 (Fig. 7c) seen for PDOF A. The misuse parameter X_5 (far side harness slack) is found to be singularly insignificant for the determination of Neck Moment in side impact crash. However, cross interactively, three observations namely X_1X_5, X_3X_5, X_5X_6 of moderate significance are noted of which only the first is from PDOF B whilst the last two are exclusively from PDOF A. The respective Response Surface plots are shown in Fig. 6b, 7c and d. Similar to X_5, the X_6 parameter (near side harness slack) has no singular significance, but retains some cross interactivity across the models. The PDOF B group has only one cross interaction parameter, X_1X_6 (Fig. 6c) while PDOF A reveals two observations X_2X_6 (Fig. 7a) and X_5X_6 (Fig. 7d), all of moderate significance.

Finally, a study of Fig. 4 shows that for some parameters, diametrically opposite effects are noted in the NM response for different PDOF groups i.e., NM is reduced rather than increased for the same parameters in different PDOF groups. This is most notable in the single and quadratic pair of parameter X_1. This occurrence is also present in X_4X_5 and all cross interaction parameters of X_2. In general, this strongly suggests the nature of these parameters effect influencing the NM to be highly sensitive to impact angle classification range groups.

CONCLUSION

Response Surface Models have been generated using LHS design and has been shown to have good fitness. Parametric behavior affecting Neck Moments during side impact crash affecting restrained child, which is previously unavailable, is captured. The singular and cross interactive parameter sensitivity for Neck Moments in a 3 year old child involved in intrusive side impact at standard test impact speed of 32.2 km/h is studied and acceptable values of the t statistic and its significance p are obtained and reported.

The number of significant parameters affecting the Neck Moment is shown to be largest for wide impact angles (ϕ≥60°) and the PDOF angle X_1 is largely revealed to be the most sensitive parameter and on which all the other remaining parameters are highly dependent on. An ideal safe range for low NM has been established to be within ϕ angles 42° and 60°. The results show X_1 having an increasing effect on NM at wide impact angles, while a decreasing effect is seen for narrow impact angles. The other parameters are generally found to be moderately significant only for wide PDOF impact angles. The harness friction coefficient (X_4) has been found to hold relatively very little effect on NM. In conclusion, the oblique side impact with intrusion affects the Neck Moment very differently compared to purely lateral crash.

ACKNOWLEDGMENT

REFERENCES

Anderson, M., K. Arbogast, B. Pipkorn and P. Lovsund, 2011. Characteristics of crashes involving injured children in side impacts. Int. J. Crashworthines., 16:4(2011): 365-373.

Arbogast, K., I. Chen, D. Durbin and F. Winston, 2004. Child retraints in side impacts. Proceeding of the International Conference on the Biokinetics of Impact. Graz, Austria.

Arbogast, K.B., Y. Ghati, R.A. Menon, S. Tylko, N. Tamborra and R.M. Morgan, 2005. Field investigation of child restraints in side impact crashes. Traffic Inj. Prev., 6(4): 351-360.

Decina, L.E. and K.Y. Knoebel, 1996. Patterns of misuses of child safety seats. Report DOT HS 808 440, National Highway Traffic Safety Administration, Washington, DC.

ECE R95-Reg 95, Year. Uniform Provisions Concerning the Approval of Vehicles with Regard to the Protection of the Occupants in the Event of a Lateral Collision. United Nations Economic Commision for Europe. Retrieved from: http://www.unece.org/ fileadmin/DAM/trans/main/ wp29/wp29regs/r095a4c1e.pdf.

FMVSS (Federal Motor Vehicle Safety Standards), 2013. 2013-child Restraint Systems. Standard No. 213, US Department of Transportation. Retrieved from: http://www.fmcsa.dot.gov/rules-regulations/ administration/ fmcsr/ fmcsrruletext.aspx?reg= 571.213.

Heiko, J., G. Barley, S. Carine, P. Claeson, L. Bjorn, K. Nojiri, F. Renaudin, L. van Rooij and A. Siewertsen, 2007. Review of the development of the ISO side impact test procedure for child restraint systems. Proceeding of the 20th ESV Conference. Lyon, France.

Howard, A., L. Rothman and M. McKeag, 2004. Children in side impact motor vehicle crashes: Seating position in injury mechanism. J. Trauma, 56(2004): 1276-1285.

Kapoor, T., W. Altenhof, A. Howard, J. Rasico and F. Zhu, 2008. Methods to mitigate injury to toddlers in near-side impact crashes. Accident Anal. Prev., 40: 1880-1892.

NHTSA, 2002. Advanced Notice of Proposed Rulemaking (ANPRM). 49 CFR Part 571 Docket No. 02-12151, RIN 2127-AI83 FMVSS 213. Retrieved from: http://www.nhtsa.gov/cars/rulings/CPSUpgrade/CPSSide/Index.htm.

NHTSA, 2007. NHTSA Vehicle Crash Test Database. Test No. 4585. Retrieved from: http://www.nrd.nhtsa.dot.gov/database/aspx/vehdb/querytesttable.aspx (Accessed on: August, 2007).

NHTSA (National Highway Traffic Safety Administration), 2005. Traffic Safety Facts 2005. DOT HS 810 61, U.S. Department of Transportation, pp: 1-6.

Shasthri, S., Q. Shah, V. Kausalyah, M. Idres, K. Abdullah and S.V. Wong, 2013. Lateral side impact crash simulation of restrained 3 year old child. Proceeding of the 2nd International Conference on Recent Advances in Automotive Engineering and Mobility Research. K.L., Malaysia, Dec. 16-18, 2013.

Starnes, M. and A.M. Eigen, 2002. Fatalities and injuries to 0-8 years old passenger vehicle occupants based on impact attributes. Report No. DOT HS 809 410, NHTSA, Washington, DC.

Statistics Canada, 2003. Major Causes of Death. Government of Canada. Retrieved from: http://142.206.72.67/02 /02b /02b_003_e.htm. (Accessed on: February, 2007).

TNO, 2013. TNO Automotive. MADYMO Manual Version 7.4.1. Delft, Netherlands.

Wang, Q., T. Kapoor, M. Tot, W. Altenhof and A. Howard, 2007. Child restraint seat design considerations to mitigate injuries to three-year-old children in side impact crashes. Int. J. Crashworthines, 12(6): 629-644.

Weber, K., 2000. Crash protection for child passengers: A review of the best practice. UMTRI Res. Rev., 31(3): 1-28. Retrieved from: http://www.umtri.umich.edu/library/pdf/webe.pdf (Accessed on: 31 July-September, 2000).